

Martin R. Johnson<sup>1</sup>

*Trinapco, Inc., 1101 57<sup>th</sup> Avenue, Oakland CA USA 94621*

**Abstract:** Special relativity’s constant speed of light ( $c$ ) means that proper distance ( $d$ ) and photon travel time ( $t_i$ ) are collinear. Isotemporal or ‘instant’ radial recession rate  $v$  of a star connects to a Hubble parameter  $H$ . A ‘Lorentz wall’ ( $c/H$ ) is defined. The product of the wall and  $v/c$  ( $\beta$ ) gives a lesser ‘Lorentz distance’ ( $d_L$ ) which cannot reach or cross the wall. Proper  $d$  is an instant product of the Lorentz distance and the Lorentz factor ( $\gamma$ ). For any  $\Lambda$ CDM-based  $H$ , there is an instant  $\beta$  whose star’s Lorentz distance is identical to its calculated observed distance at the same  $H$ . This  $\beta$  is found from the star’s observed cosmic redshift. Distant rest mass’s elapsed time upon our reception of its photons is known as ‘lookback’ and herein proposed as another instant product, of the Lorentz distance and the Lorentz factor squared (when divided by  $c$ ). Type 1a supernovae with Phillips behavior display increased decay times at higher  $z$ . The present paper proposes nonlinear  $z$  dependence on these decay times. This may improve constraint on model parameters.

## 1 INTRODUCTION

Determination of a star’s Hubble parameter  $H$  involves two measurements: Cosmic redshift  $z$  and observed distance  $d_{obs}$ . Much progress has been made since Vesto Slipher’s first observation of  $H$  (Slipher 1917). The efforts of many astronomers over the last century, now including the vast trove of data from DESI (Allali 2025)(Adame 2025), give potential  $H$  measurements numbering in the millions. Type 1a supernovae have the most consistent behavior, but are less numerous. These are aggregated to produce simple models of  $H$  as a function of  $z$ . Since 1998 (Perlmutter)(Riess), the standard model has been  $\Lambda$ CDM, presently under fire from DESI. This paper does not delve into the controversy (Ye 2025) surrounding the tension between  $\Lambda$ CDM and DESI’s findings. We will use the  $\Lambda$ CDM model only as a proxy for observations to date. We can deduce a fundamental principle of stellar observation through  $\Lambda$ CDM without resort to extensive comparison with large datasets. This fundamental principle is the Lorentz effect. The present author suggests that Lorentz contraction is built into observed  $H$ . Its effect on  $d_{obs}$  is a core property, and will apply to any more accurate distance-ladder model that may arise.

---

<sup>1</sup> E-mail: [ceo@trinapco.com](mailto:ceo@trinapco.com). ORCID 0000-0002-5096-3206

We first explore the concept of an ‘instant flat Universe’, Euclidean at scale and frozen in time. We then connect its instant behavior to the observed Universe, which looks back in time. The Lorentz effect plays a central role in both.

Most of the present paper’s content is well known and found in introductory texts, e.g. (Ryden 2017)(Liddle 2015)(Huterer 2023)(Baumann 2022), to which the reader is referred. Herein we define ‘proper distance’ as the distance traveled by a photon from source to receptor. This definition differs from the texts.

## 2 LORENTZ EFFECTS IN THE INSTANT UNIVERSE

In Einstein’s theory of special relativity, proper distance  $d$  and photon travel time  $t_\lambda$  are connected by the speed of light  $c$ . They are collinear:

$$c = \frac{d}{t_\lambda} \quad (1)$$

Under the Cosmological Principle, at any point in time  $t$ , the instant Universe at very large scale is generally considered by the texts as having been perfectly ‘flat’ over all  $t$ , with Euclidean geometry in both Cartesian  $x,y,z$  and radial  $d,\theta,\phi$  coordinates. We use this flat hypothesis.

A scalar Hubble parameter  $H$  is applied to the instant coordinates:

$$H = \frac{v}{d_L} \quad (2)$$

Where  $v$  is the radial recession rate between two points (us and a star). The *Lorentz distance*  $d_L$  depends on  $v$ . When  $v \ll c$ , Lorentz effects are negligible;  $d_L = d$ . As  $v \rightarrow c$ , Lorentz contraction ‘shortens’  $d_L$ :

$$d_L = d \sqrt{1 - \frac{v^2}{c^2}} = d \sqrt{1 - \beta^2} = \frac{d}{\gamma} \quad (3)$$

Where  $\beta = v/c$ , and  $\gamma$  is the Lorentz factor:

$$\gamma = \frac{1}{\sqrt{1 - \beta^2}} \quad (4)$$

When  $\beta = 0.001$ ,  $d_L = 0.9999995d$ . Proper  $d$  and  $d_L$  are effectively the same.

We partition the  $d$  line into proper  $d_{seg}$ ’s, each with  $\beta_{seg} = 0.001$ , and assign an origin point or *rest frame*. All the  $d_{seg}$ ’s have the same speed  $v_{seg} = \beta_{seg}c$ . These add to give a serial  $v_L$ :

$$v_L = \sum \beta_{seg}c \quad (5)$$

The  $d_{seg}$ ’s don’t just add. They give a serial  $d_L$  whose sequential  $d_{seg}$ ’s become ‘shorter’ at the origin as they grow more distant:

$$d_L = \sum \frac{d_{seg}}{\gamma_{seg}} \quad (6)$$

When you move the rest frame along the  $d$  line, distant and ‘shorter’  $d_{seg}$ ’s on one side get closer, and stretch back out to their proper length. The  $d_{seg}$ ’s on the other side grow more distant. They become ‘shorter’.

Serial  $d_L$  approaches a *Lorentz wall*  $W_L$  (Figure 1) as the  $d_{seg}$ ’s cumulative  $v_L \rightarrow c$ :

$$W_L = \frac{c}{H} \quad (7)$$

The last  $d_{seg}$  cannot give  $v \geq c$  (if Einstein was right). This creates a gap  $[W_L - d_L]$  which must be filled with proper  $d_{seg}$ ’s  $\rightarrow 0$ . There is no upper boundary on  $d$  itself: As  $v \rightarrow c$ ,  $d \rightarrow \infty$ .

A more tractable approach to Eq. (6) is linear in  $\beta$ :

$$d_L = W_L \beta \quad (8)$$

From Eqs. (3) and (8), proper distance  $d$  is thus:

$$d = d_L \gamma = W_L \beta \gamma = \frac{c \beta \gamma}{H} \quad (9)$$

Table 1 gives some instant  $d$  values as  $\beta \rightarrow 1$  for three different  $H$ ’s. As  $v \rightarrow c$ ,  $d_L \rightarrow W_L$  for each  $H$ . Proper  $d$ , however, increases dramatically. This is most pronounced at lower  $H$  (and  $z$ ). For today’s  $z = 0$ , with our chosen  $H_0 = 73 \text{ km s}^{-1} \text{ Mpc}^{-1}$ , the last entry in Table 1 ( $\beta = 0.9999999999$ ) gives  $d = 947,000$  gigalight-years (Glyr). At  $z = 1089$  (Bennett 2003), the time of last scattering,  $W_L$  was much less. The corresponding  $d$  is 41 Glyr. Photons from a light source receding that fast, that long ago, would take 41 billion years to see. This ‘source’ is the cosmic microwave background (CMB); there were no stars. These CMB photons would have a modal ten-kilometer wavelength by the time they reach our successors.

When we use  $\beta$  as the linear domain, the Lorentz wall  $W_L$  becomes the radius of a *Lorentz sphere* which contains the entire Universe’s kinetic energy and rest mass. Its infinite energy lies almost entirely within a thin outermost  $\beta$  shell  $[W_L - d_L]$ . Every instant Cartesian point  $x,y,z$  is surrounded by a Lorentz sphere, which contains every other point. Almost all these points are compressed into the shell. The sphere’s coordinates  $\beta,\theta,\phi$  constitute dimensionless *Lorentz space* which has physical meaning via  $H$  and  $c$ . The points  $\beta,\theta,\phi$  are only transposable with the sphere’s center or rest frame, and not each other. Any  $\beta > 1$  in Lorentz space is unphysical.

The Lorentz sphere’s finite radius  $W_L$  means that we can talk about the Universe having a finite ‘size’. It was much ‘smaller’ long ago than today. However, if perfectly flat, the Universe is unbound in  $d$ , and has always been infinitely large in Euclidean space. It’s just been getting less

dense. In the texts, today's wall  $W_{L_0} = c/H_0$  is called the 'Hubble distance'. The term 'horizon' is also used.

### 3 LORENTZ EFFECTS IN THE OBSERVED UNIVERSE

We now examine the observed Universe. In section 3.1, we connect  $d$  to  $\Lambda$ CDM's calculated distance  $d_\Lambda (\equiv d_{obs})$ . The ' $\Lambda$ ' subscript refers to  $\Lambda$ CDM *in toto*. In section 3.2, we calculate lookback ( $t_0 - t$ ) via  $t_\lambda$ . By inclusion of Lorentz effects, we will see how high-redshift luminous objects can appear both closer and older than predicted by  $\Lambda$ CDM alone.

#### 3.1 Proper distance vs. cosmic redshift

A star's observed redshift  $z$  gives its  $\beta$ :

$$\beta = \frac{(z+1)^2 - 1}{(z+1)^2 + 1} \quad (10)$$

Combining Eqs. (4) and (10) gives  $\gamma(z)$ :

$$\gamma = \sqrt{\frac{1}{2}z^2 + z + 1} \quad (11)$$

The 'minimum flat-Universe'  $\Lambda$ CDM model is:

$$H = \frac{v}{d_\Lambda} = \frac{\beta c}{d_\Lambda} = H_0 \sqrt{\Omega_{\lambda_0}(z+1)^4 + \Omega_{(b+c)_0}(z+1)^3 + \Omega_{\Lambda_0}} \quad (12)$$

Most term values in Eq. (12) are given in Table 1. The remaining  $d_\Lambda$  term is a  $z$ -dependent aggregate of individual distances  $d_{obs}$  derived from measurement of luminosity and/or angular size of the source. Recession rate  $v$  is, in general, more precisely found than is  $d_\Lambda$  for each measurement. Table 1 gives selected results using Eqs. (9) – (12). We can see that the  $\Lambda$ CDM-calculated  $d_\Lambda$  and Lorentz  $d_L$  distances are identical to 20 ppm for any instant  $z$ . The miniscule error is itself constant out to nine decimal places. Such precise and accurate identification suggests that what we see through a telescope is Lorentz-contracted. To get the proper distance, we can use  $d_\Lambda$  instead of  $d_L$  in Eq. (9). Combining Eqs. (9) - (12) gives:

$$d = d_\Lambda \gamma = d_\Lambda \sqrt{\frac{1}{2}z^2 + z + 1} \quad (13)$$

Equation (13) returns a surprising result: Proper distance between source and receptor reached a maximum at  $z = 1.6$ , when  $d = 6$  Glyr. Luminous bodies at  $z > 1.6$  were *actually closer* than they were at  $z = 1.6$ . They got even more close as  $z$  rises further. This explains why high- $z$  stars and galaxies can appear brighter and larger, e.g. (Naidu 2022), than  $\Lambda$ CDM's prediction. See (Gupta 2023) for a longer list. Received photon flux and observed angular distance are reduced (or enhanced) by an increase (or decrease) in proper distance upon emission. Stars and galaxies get

larger and brighter, or smaller and fainter, depending on whether  $\partial d/\partial z$  is negative or positive. Intervening dust and/or general relativistic lensing can affect observed size.

Equation (13)'s nonmonotonic variance of  $d$  with  $z$  was inconsistent with the present author's then-belief that stars at higher redshift should have been further away. This confounding state of affairs clarified, after author acquired a better understanding of lookback.

### 3.2 Lookback vs. cosmic redshift

Lookback ( $t_0 - t$ ) is elapsed cosmic time between source ( $-t$ ) and receptor ( $t_0$ ). In this subsection, the author endeavors to show that lookback has monotonic variance with redshift. Stars at  $z > 1.6$  may have grown ever closer to us, but they were also ever older.

Lookback approaches  $t_\lambda$  only if the source is receding at  $\beta \ll 1$ . When recession is fast enough, elapsed time at the receptor (us) drops in our rest frame, by  $\gamma^{-1}$ . Elapsed time at the source is given by Eq. (14):

$$(t_0 - t) = t_\lambda \gamma \tag{14}$$

For example, a rest source can have light pulses at a rate one per second. If the source is receding at  $\beta = 0.998611$ , when those pulses reach us, the rate we see drops sixtyfold, to one per minute. It doesn't matter how far away the source was, is, or will be. As long as it's moving away from us at that same radial velocity, the light pulses will be slowed down to one per minute. In the source's rest frame, it's us, the receptor, that has slowed down. We know that our light pulses are one second apart, so we have to speed things up on the other end to get an accurate calculation of elapsed source time since emission. Equation (14) does this. Cosmic time comoves at about the same rate in either frame. If the source is another Earth mass, then elapsed cosmic times become more nearly identical in both frames.

For a source with constant  $\beta$ , Eq. (14) applies to any proper  $d$ . The author believes that Eq. (14) remains an accurate description of elapsed time at the source with variant  $\beta$  as well. Once that photon is emitted, any later change in the source's  $\beta$  doesn't change the photon's  $t_\lambda$ . Change in  $\beta$  would affect the source's age *after* emission, but for our purposes, we are only interested in its instant age. The present author asks the reader to consider the possibility that elapsed time at the source can be expressed as an instant product, and Eq. (14) applies to any instant  $z$ . In the texts, line integration is used to adjust for the 'expansion of space' and its purported effect on lookback and proper distance. This concept of the 'expansion of space' is widespread in the literature. Such 'expansion' corresponds to off-center point transposition in Lorentz space. Herein,  $t_\lambda$  is preferred for lookback calculation. When Lorentz effects are factored into  $t_\lambda$  and  $d_\lambda$ , numeric integration along  $\partial z$  simply returns the same results as the instant Eqs. (14) and (13) respectively (see supporting information). Line integration remains useful for e.g. estimating dust interference in the photons' travel path, and for the general relativistic effect on comoving cosmic time in the

very early Universe. This latter effect underpins inflation (Guth 1981), a subject of less interest to the practicing astronomer.

Combining Eqs. (1), (13), and (14) gives:

$$(t_0 - t) = \frac{d_A}{c} \left( \frac{1}{2} z^2 + z + 1 \right) \quad (15)$$

Figure 2 shows the range of Eqs. (7), (8), (9), and (15) for  $z = 0 \rightarrow 20$ . Table 2 gives Figure 2's numbers at selected  $z$ 's. At  $z = 5$ , Eq. (15) gives a  $\Lambda$ CDM 'universe' 14.6 Gyr older than today. At  $z = 20$ , it's 27.5 Gyr. At  $z = 1089$ , those photons from the CMB reached us after only 0.317 Gyr, but their 'source' was  $\approx 173$  Gyr older than that. The 173 Gyr value uses  $H_0 = 73$  ( $\text{km s}^{-1} \text{Mpc}^{-1}$ ) (Riess 2024a). Using  $H_0 = 68$  instead (Planck 2020), Eq. (15) gives  $(t_0 - t)_{1089} = 186$  Gyr. Back then, baryons can be consistently described as having been an isotropic, un-ionized, and monatomic gas. Equation (15) allows plenty of time afterward for galaxy evolution.

When Eq. (15) is multiplied by  $c$ , we get the *static distance*, which would be the proper distance in a noncomoving or static 'universe'. The Universe comoves, so static distance is unphysical. Equations (11) and (14) do usefully connect certain supernova decay times with  $z$ .

### 3.3 Decay times of type 1a supernovae

Type 1a supernovae (SN's) (Howell 2011) are brilliant and ephemeral, having consistent rise-and-fall profiles which follow a (luminosity) – (decay time) relation (Phillips et al. 1993)(Hamuy et al. 1995). These SN's are presently divided into 1a subtypes, of which  $\approx 70\%$  (Liu et al. 2023) still follow the Phillips-Hamuy relation. Recent observation (Riess et al. 2024b) of these transient events using the JWST telescope have strengthened the distance ladder, and reaffirmed the Hubble tension. Much effort has been expended by these and other authors toward systematic exclusion of nearby light source interference after SN candidate capture and assignment. This exclusion process was helped considerably by JWST's deployment in 2021, with its extended infrared detection range and large mirror. The Riess group's JWST observations added another sixteen SN's to the original 42 SN dataset of the Perlmutter group (Perlmutter et al. 1999).

Distance (found from brilliance) and recession (found from redshift) of these SN's have time- and wavelength- dependent variances which require correction to a baseline rise-and-fall profile. These corrections allow for the interwoven effects of the Phillips-Hamuy relation, Galactic extinction, cosmic redshift, wavelength-dependent U-B-V-R-I brilliance, low- $z$  peculiar motion, hypothetical red and grey dust interference, time dilation, and any other factors this author may have overlooked. Peak brilliance, or magnitude  $m$ , is held as dominated by the  $^{56}\text{Ni} \rightarrow ^{56}\text{Co} \rightarrow ^{56}\text{Fe}$  beta cascade inside the SN. The cascade gives two decay half-lives  $t_1 \rightarrow ^{56}\text{Co}$  (6.1 days) and  $t_2 \rightarrow ^{56}\text{Fe}$  (77 days) respectively. The former ( $t_1$ ) is brighter and principal. Observation of the latter ( $t_2$ ) is convoluted by longer-lived and less-energetic decay events within the SN. These

half-lives combine with the Phillips-Hamuy relation to give a baseline. Their  $t_1$  and  $t_2$ 's are affected by time dilation, which we now examine.

Cosmic redshift affects the UBVRI profile: U→B→V, etc. Recession rate is calculated from a best fit of these ‘stretched’ spectra to Eq. (10). Distance is found from bolometric  $m$  via *inter alia* addition of a ‘stretch factor’  $s = (z + 1)$  to e.g. the B band  $m_B$  (Perlmutter 1999):

$$m_B^{corr} = m_B + \Delta_{corr}(s) \quad (16)$$

Where  $m_B^{corr}$  is the corrected (increased) peak magnitude, and  $\Delta_{corr}(s)$  is given by:

$$\Delta_{corr}(s) = \alpha(s - 1) = \alpha z \quad (17)$$

The  $\alpha$  term is a monotonic function. Equation (16) treats time dilation as additive with  $z$ . This results in  $t_1$  and  $t_2$  increases which do not remain proportional. The present author takes issue, as it is inconsistent with Eq. (14). In lieu of Eqs. (16) and (17), author suggests:

$$m_B^{corr} = m_B \alpha_\gamma \gamma = m_B \alpha_\gamma \sqrt{\frac{1}{2}z^2 + z + 1} \quad (18)$$

Equation (18) lengthens the decay times proportionally. The  $\alpha \rightarrow \alpha_\gamma$  function is now a dimensionless bolometric ratio:

$$\alpha_\gamma = \frac{\int_{\lambda=0}^{\infty} E_{\lambda_\gamma} \partial \lambda}{\int_{\lambda=0}^{\infty} E_{\lambda_0} \partial \lambda} \quad (19)$$

The  $E_\lambda$  terms give total photon energy at any one wavelength. Equation (19) expresses the relative decrease in integral photon energy from  $\lambda$  stretch at any one  $\gamma$  vs. the SN’s baseline at  $\gamma = 0$ . The  $\lambda$  profile is presently observed with filters; author is unaware of any single-photon-counting  $\lambda$ -scanning instruments in use. This author is reluctant to use the Boltzmann curve for Eq. (19), as the SN’s emission profile may not follow it. Times  $t_1$  and  $t_2$  are governed by  $\gamma$  alone. Table 3 gives increases in  $t_1$  and  $t_2$  vs.  $z$ . These are the proposed numbers which should correlate with calculated  $z$  from a best-fit to the UBVRI profile. At  $z = 0.2$ , the Phillips-adjusted observed  $t_1$  and  $t_2$  should be 6.7 and 85 days. At  $z = 0.5$ , they should be 7.8 and 98 days. If a high- $z$  Phillips-Hamuy subtype with these  $t_1$  and  $t_2$ 's could be found by JWST at e.g.  $z = 4$ , then they would be 22 and 278 days respectively. These numbers may help provide more accurate parameter constraint at higher  $z$ . This won’t, however, solve the Hubble tension. The present author believes its origin lies with Planck’s methodology (Johnson 2025).

### 3.4 General effects

The present paper does not include general relativistic effects. One publication (Lorenz 2018) suggests that general effects at cosmic scale are negligible, with only local impact on observation of overdense regions in the Universe. Underdense regions are unaffected. This author concurs.

## 4 CONCLUSION

The present paper gives proper distance  $d$  as an instant product. Lookback ( $t_0 - t$ ) is herein proposed as another instant product. Both are calculable without line integration. This paper's findings do not obviate a model's dependence of  $H$  on aggregate  $d_{obs}$ . They do, however, provide needed corrections for estimates of  $d$  and ( $t_0 - t$ ). The key concept that the author emphasizes is faithful adherence to special relativity's constant speed of light in a perfectly flat Universe. Recession speeds are properly found in Lorentz space from its rest frame at the Lorentz sphere's center, rather than arbitrary two-point transposition in flat Euclidean space away from our rest frame. Both Lorentz and Euclidean instant coordinate recessions can never exceed  $c$ .

## REFERENCES

- Adame et al., 2025, [J. Cosmol. Astropart. Phys. 2025, 012](#).
- Allali, I. J., Notari, A., & Rompineve, F., 2025, [J. Cosmol. Astropart. Phys. 2025, 023](#)
- Baumann, D., 2022, [Cosmology](#).
- Bennett, C. L., et al., 2003, [ApJ Supp. Ser., 148, 1](#).
- Gupta, R. P., 2023, [MNRAS, 524, 3385](#).
- Guth, A. H., 1981, [Phys. Rev. D, 23, 347](#).
- Hamuy, M., et al., 1995, [AJ, 109, 1](#).
- Howell, D. A., 2011, [Nature communications 2, 350](#).
- Huterer, D., 2023, [A course in cosmology](#).
- Johnson, M. R., 2024, J. Subatomic Part. & Cosmol., JSPC-D-24-00041, [submitted](#).
- Liddle, A., 2015, An introduction to modern cosmology, Oxford press, ISBN 978-1-118-50214-3.
- Liu, Z-W., Röpke, F. K., & Han, Z., 2023, [R. Astron. Astrophys., 23, 082001](#).
- Lorenz, C. S., Alonso, D., & Ferreira, P. G., [Phys. Rev. Lett., 97, 023537](#).
- Naidu, R. P., et al., 2022, [ApJ lett., 940, 1](#).
- Perlmutter, S., et al., 1998, [Nature 391, 51](#).
- Perlmutter, S., et al., 1999, [ApJ, 517, 565](#).

Phillips, M. M., 1993, [ApJ, 413, L105](#).

Planck et al., 2020, [A&A, 641, A1](#).

Riess, A. G., et al., 1998, [ApJ 116, 1009](#).

Riess, A. G., et al., 2024a, [ApJ lett., 962, L17](#).

Riess, A. G., et al., 2024b, [ApJ, 977, 120](#).

Ryden, B., 2017, [Introduction to cosmology, second edition](#).

Slipher, V. M., 1917, [The Observer, 40, 304](#)

Ye, G., Martinelli, M., Hu, B., & Silvestri, A. 2025, [Phys. Rev. Lett. 134, 181002](#).

TABLE 1: Instant Lorentz and proper distances vs. $\beta$ , for selected $z$ and $\Lambda$ CDM $H$ values*						
Cosmic redshift:	$z = 0$		$z = 10$		$z = 1089$	
$\Lambda$ CDM $H$ , Gyr <sup>-1</sup> :	0.07465		1.518		1,716.0	
$W_L$ , Gyr:	13.395814		0.658797		0.000583	
$\beta$	$d_L$ , Gyr	$d$ , Gyr	$d_L$ , Gyr	$d$ , Gyr	$d_L$ , Gyr	$d$ , Gyr
0.01	0.134	0.134	0.00659	0.007	0.000006	0.000006
0.1	1.340	1.346	0.0659	0.066	0.000058	0.000059
0.5	6.698	7.734	0.329	0.380	0.000291	0.000336
0.9	12.06	27.7	0.593	1.36	0.000524	0.00120
0.99	13.26	94.0	0.652	4.62	0.000577	0.00409
0.999	13.38	299	0.658	14.7	0.000582	0.0130
0.9999	13.394	947	0.6587	46.6	0.000582	0.0412
0.99999	13.3957	2,995	0.658790	147	0.000583	0.130
0.999999	13.3958	9,472	0.658796	466	0.000583	0.412
0.9999999	13.395812	29,954	0.658797	1,473	0.000583	1.3022
0.99999999	13.395813	94,722	0.658797	4,658	0.000583	4.119
0.999999999	13.395814	299,539	0.658797	14,731	0.000583	13.02
0.9999999999	13.395814	947,227	0.658797	46,584	0.000583	41.19

\*  $\Lambda$ CDM parameters:  $H_0 = 73.00 \text{ Km s}^{-1}\text{Mpc}^{-1}$  (Riess 2024a).  
Others from (Planck):  $\Omega_{(b+c)} = 0.3091$ ;  $\Omega_{\lambda_0} = 0.000091 \pm 0.000005$ ;  $\Omega_A = 0.6908$ .

TABLE 2.  $\Lambda$ CDM distance, Lorentz distance, tension, tension error, and proper distance.

$z$	$d_A$	$d_L$	$d_A/d_L$	$(d_A - d_L)/d_L$	$d(= d_A\gamma)$
	Glyr	Glyr			Glyr
0.01	0.132671	0.132668	1.000021	2.053388090E-05	0.1327
0.1	1.212392	1.212367	1.000021	2.053388090E-05	1.2179
0.2	2.182471	2.182426	1.000021	2.053388090E-05	2.2188
0.5	3.912135	3.912054	1.000021	2.053388090E-05	4.2381
0.6	4.195630	4.195544	1.000021	2.053388090E-05	4.6675
0.7	4.377932	4.377842	1.000021	2.053388090E-05	5.0088
0.8	4.480904	4.480812	1.000021	2.053388090E-05	5.2774
0.9	4.522642	4.522550	1.000021	2.053388090E-05	5.4866
1	4.517814	4.517721	1.000021	2.053388090E-05	5.6472
1.1	4.478121	4.478029	1.000021	2.053388090E-05	5.7681
1.2	4.412790	4.412699	1.000021	2.053388090E-05	5.8569
1.3	4.329025	4.328936	1.000021	2.053388090E-05	5.9193
1.4	4.232408	4.232321	1.000021	2.053388090E-05	5.9605
1.5	4.127233	4.127148	1.000021	2.053388090E-05	5.9844
1.6	4.016779	4.016697	1.000021	2.053388090E-05	5.9941
1.7	3.903536	3.903456	1.000021	2.053388090E-05	5.9925
1.8	3.789375	3.789298	1.000021	2.053388090E-05	5.9817
1.9	3.675692	3.675617	1.000021	2.053388090E-05	5.9634
2	3.563511	3.563438	1.000021	2.053388090E-05	5.9391
3	2.610761	2.610707	1.000021	2.053388090E-05	5.5478
4	1.970316	1.970275	1.000021	2.053388090E-05	5.1227
5	1.541486	1.541454	1.000021	2.053388090E-05	4.7528
6	1.243610	1.243585	1.000021	2.053388090E-05	4.4414
7	1.028614	1.028593	1.000021	2.053388090E-05	4.1787
8	0.868139	0.868121	1.000021	2.053388090E-05	3.9548
9	0.744915	0.744900	1.000021	2.053388090E-05	3.7617
10	0.648010	0.647997	1.000021	2.053388090E-05	3.5934

TABLE 3. SN1a $t_1$ and $t_2$ increase with redshift, from Eq. (18)						
$z$	$t_1$ , days	$t_2$ , days		$z$	$t_1$ , days	$t_2$ , days
0	6.1	77		1.3	10.82	136.55
0.1	6.41	80.94		1.4	11.21	141.56
0.2	6.74	85.05		1.5	11.61	146.60
0.3	7.07	89.30		1.6	12.02	151.67
0.4	7.42	93.67		1.7	12.42	156.77
0.5	7.78	98.16		1.8	12.82	161.88
0.6	8.14	102.73		1.9	13.23	167.02
0.7	8.51	107.39		2	13.64	172.18
0.8	8.88	112.11		2.5	15.70	198.19
0.9	9.26	116.90		3	17.78	224.49
1	9.64	121.75		3.5	19.88	250.99
1.1	10.03	126.64		4	21.99	277.63
1.2	10.42	131.58		5	26.24	331.19

Figure 1. The Lorentz wall  $W_L$   
( $\gamma \rightarrow \infty$  as  $\beta \rightarrow 1$ )

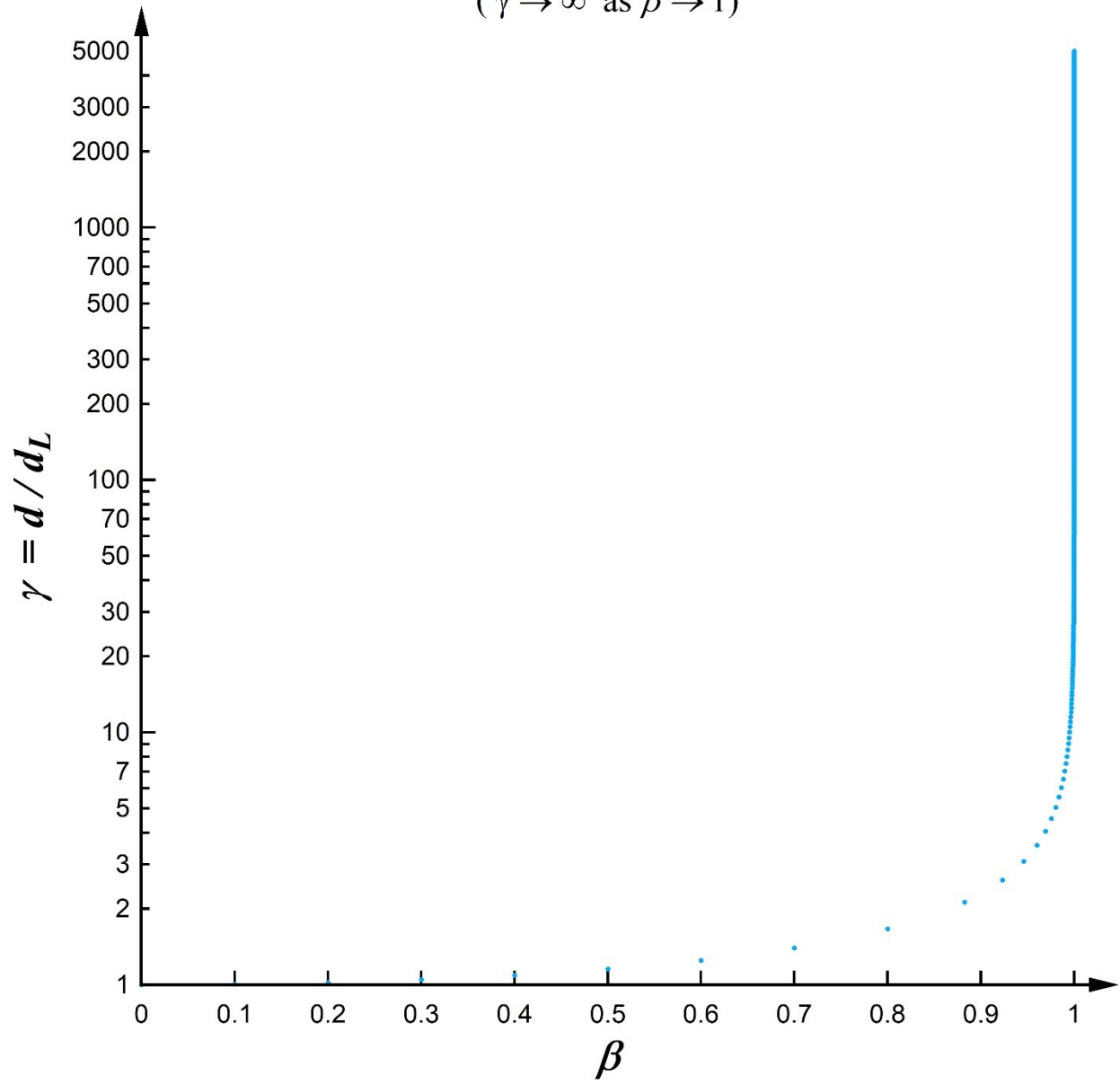


Figure 2. Lorentz wall, observed and proper distances, and lookback vs. redshift

